Published in final edited form as:
Science. 2021 July 09; 373(6551): 231–236. doi:10.1126/science.abg2264.

An isoform of Dicer protects mammalian stem cells against multiple RNA viruses

Enzo Z. Poirier[1,*], **Michael D. Buck**[1], **Probir Chakravarty**[2], **Joana Carvalho**[3,4], **Bruno Frederico**[1], **Ana Cardoso**[1], **Lyn Healy**[5], **Rachel Ulferts**[6], **Rupert Beale**[6,7], **Caetano Reis e Sousa**[1,*]

[1]Immunobiology laboratory, The Francis Crick Institute, London NW1 1AT, UK

[2]Bioinformatics & Biostatistics, The Francis Crick Institute, London NW1 1AT, UK

[3]Experimental Histopathology, The Francis Crick Institute, London NW1 1AT, UK

[4]Current address: Histopathology Scientific Platform, Champalimaud Centre for the Unknown, Avenida Brasilia, 1400-038 Lisboa, Portugal

[5]Human Embryo and Stem Cell unit, The Francis Crick Institute, London NW1 1AT, UK

[6]Cell Biology of Infection laboratory, The Francis Crick Institute, London NW1 1AT, UK

[7]Division of Medicine, University College London, London WC1E 6BT, UK

Abstract

In mammals, early resistance to viruses relies on interferons, which protect differentiated cells but not stem cells from viral replication. Many other organisms rely instead on RNA interference (RNAi) mediated by a specialised Dicer protein that cleaves viral double stranded RNA. Whether RNAi also contributes to mammalian antiviral immunity remains controversial. We identified an isoform of Dicer, named antiviral Dicer (aviD), that protects tissue stem cells from RNA viruses —including Zika virus and severe acute respiratory syndrome coronavirus 2 (SARS-CoV-2)— by dicing viral double-stranded RNA to orchestrate antiviral RNAi. Our work sheds light on the molecular regulation of antiviral RNAi in mammalian innate immunity in which different cell-intrinsic antiviral pathways can be tailored to the differentiation status of cells.

Type I and III innate interferons (IFNs) are rapidly induced in mammalian cells in response to virus infection. These cytokines act in autocrine and paracrine manner to promote the transcription of multiple interferon stimulated genes (ISGs), which encode a variety of viral restriction, cellular arrest, and cell death factors (1). The inducible protection conferred by IFN receptor signalling is much more marked in differentiated cells than in embryonic and

*Correspondence: EZP (enzo.poirier@crick.ac.uk) or CRS (caetano@crick.ac.uk).

Author contributions: EZP and CRS designed experiments and analysed data. EZP conducted experiments with the assistance of MDB, AC, BF and LH. JC performed the BaseScope *in situ* hybridization experiment and PC analysed the small RNA sequencing data. RU and RB provided SARS-CoV-2 reagents. EZP, MDB and CRS wrote the manuscript. CRS supervised the project.

Competing interests: CRS has an additional appointment as Professor in the Faculty of Medicine at Imperial College London and owns stock options and/or is a paid consultant for Bicara Therapeutics, Montis Biosciences, Oncurious NV, Bicycle Therapeutics and Sosei Heptares, all unrelated to this work. The remaining authors declare no competing interests.

Europe PMC Funders Author Manuscripts

adult stem cells, which lack expression of components of the pathway that leads to IFN induction and that which confers IFN responsiveness (2–4). This may ensure that infected stem cells are spared the cytostatic and cytotoxic effects of IFN exposure.

The IFN system is absent from invertebrates and plants, which protect themselves from viral infection by means of RNA interference (RNAi) (5). Antiviral RNAi starts with the protein Dicer, which recognizes and cleaves double-stranded RNA (dsRNA) produced during RNA virus infection to generate small interfering RNAs (siRNAs). These guide the sequence-specific degradation of viral RNAs by a slicing-active Argonaute protein such as Argonaute 2 (Ago2), present in insects and mammals. Irrespective of infection, RNAi also has a distinct role in regulating cellular gene expression, through microRNAs (miRNAs) produced by Dicer cleavage of precursor miRNAs (pre-miRNAs) (5). Recent work suggests that mammals, like invertebrates and plants, can co-opt RNAi for antiviral immunity (5). Examples of mammalian antiviral RNAi *in* vitro and *in vivo* have been reported for Nodamura virus, human enterovirus 71, Zika virus and other RNA viruses (6–14) although other studies have argued against the existence of such a response (15–18). Part of the controversy may relate to the fact that IFN inhibits mammalian dsRNA-mediated RNAi and the latter may therefore only be relevant in cells that are hyporesponsive to IFNs such as stem cells (5, 19, 20). Notably, stem cells can resist virus infection, which has been partly attributed to IFN-independent constitutive expression of restriction factors (21). Whether stem cells additionally possess specialisations that favour antiviral RNAi remains unclear.

Plants and insects that use RNAi both as a means of regulating translation of cellular mRNAs and as an antiviral mechanism encode multiple Dicers, each dedicated to one arm of the pathway. In contrast, mammals possess a single *DICER* gene with one canonical protein product, which cleaves pre-miRNA but processes dsRNA poorly (22, 23). Interestingly, a truncated form of Dicer with improved antiviral capacity can be produced from the *Dicer* gene in mice but its expression is restricted to oocytes (24). By analogy, we hypothesized that antiviral RNAi in mammals may involve expression of an isoform of Dicer that more efficiently processes dsRNA that canonical Dicer. By performing a polymerase chain reaction (PCR) on total cDNA from mouse small intestine, we identified an alternatively spliced in-frame transcript of Dicer missing exons 7 and 8 (Fig. 1A). *In silico* translation of this transcript resulted in a truncated Dicer protein in which the central Hel2i domain of the N-terminal helicase segment is absent (Fig. 1A). For simplicity, hereafter we refer to canonical Dicer (which includes the sequences encoded by exons 7 and 8) as Dicer and its truncated form as antiviral Dicer (aviD). Using a reverse transcription quantitative PCR (RT-qPCR) assay that distinguishes *aviD* and *Dicer* mRNA, both isoforms could be detected in mouse cells, including neural stem cells, embryonic stem cells (ES cells) and a 3T3 cell line, as well as in organs from pre-weaning or adult mice (fig. S1, A to D). The *AVID* and *DICER* transcripts were also found in human ES cells, human induced pluripotent stem cells (iPSCs), and some human cell lines (fig. S1, E to H). In general, transcripts encoding aviD appeared to be less abundant than transcripts encoding full-length Dicer by at least a factor of 10 (fig. S1), explaining in part why they are not easily found in public domain RNAseq datasets. Nonetheless, they resulted in detectable protein, as immunoprecipitation using an antibody that dually recognizes Dicer and aviD demonstrated the presence of low

levels of aviD protein in mouse ES cells, human iPSCs and human embryonic kidney 293T cells (Fig. 1B) but, as expected, not in *Dicer* gene deficient (Dicer$^{-/-}$aviD$^{-/-}$) cells used as a negative control (25, 26). aviD lacks part of the helicase domain, which negatively regulates Dicer ability to process dsRNA (22, 23). Consistent with that notion, recombinant aviD produced about twice as much siRNA from synthetic dsRNA as did recombinant Dicer in an *in vitro* dicing assay (Fig. 1C). In addition, aviD was more resistant to LGP2, an ISG product that inhibits dsRNA cleavage by Dicer and is partly responsible for IFN-mediated inhibition of antiviral RNAi in differentiated mammalian cells (20) (Fig. 1D). In contrast to dsRNA cleavage, both Dicer and aviD generated equivalent amounts of *let-7a* miRNA from pre-miRNA (Fig. 1E). These results suggest that loss of the Hel2i domain does not impair the ability of aviD to process miRNA precursors but confers enhanced capacity to dice dsRNA into siRNAs, a hallmark of Dicers involved in antiviral RNAi.

To assess the ability of aviD to mediate antiviral RNAi, we complemented *Dicer* gene deficient (Dicer$^{-/-}$aviD$^{-/-}$) HEK293T “NoDice” cells (26) by stable transfection with constructs encoding FLAG-tagged Dicer or aviD to generate sublines denoted as Dicer$^{+/+}$aviD$^{-/-}$ or Dicer$^{-/-}$aviD$^{+/+}$ 293T, respectively (figs. S2A and S3). By immunofluorescence, aviD and Dicer localisation was predominantly cytoplasmic (fig. S3). Consistent with the *in vitro* pre-miRNA cleavage assays (Fig. 1E), the expression of either Dicer or aviD was sufficient to restore miRNA production to Dicer$^{-/-}$aviD$^{-/-}$ “NoDice” cells (fig. S2, B and C). We then infected Dicer (Dicer$^{+/+}$aviD$^{-/-}$) or aviD (Dicer$^{-/-}$aviD$^{+/+}$) expressing cells with Sindbis virus (SINV) or with Zika virus (ZIKV), two RNA viruses that are targets of antiviral RNAi in insects. We did not include Dicer$^{-/-}$aviD$^{-/-}$ cells in these experiments to avoid confounding effects from loss of miRNA-regulated protein expression. Notably, cells expressing only aviD displayed lower production of SINV (Fig. 2A) and ZIKV (Fig. 2B) virus progeny than did cells that only expressed Dicer. We further tested doxycycline-inducible acute expression of the proteins in the same cells. aviD but not Dicer induction impaired SINV-GFP viral replication over time, as measured by accumulation of green fluorescent protein (GFP) fluorescence (Fig. 2, C to F). This was not observed with a version of aviD that was catalytically deficient in dsRNA cleavage [aviD(CD)] (Fig. 2, C to F). These data demonstrate that aviD but not Dicer possesses antiviral function that is dependent on its catalytic domain, consistent with a role in RNAi.

Mammals encode four Ago proteins, all of which can mediate miRNA-driven gene silencing. However, only Ago2 possesses endonuclease activity to mediate target “slicing” in antiviral RNAi. Silencing Ago2 in Dicer$^{-/-}$aviD$^{+/+}$ cells (Fig. S4A) rescued ZIKV particle production to levels similar to those in Dicer$^{+/+}$aviD$^{-/-}$ cells treated with control or *Ago2* siRNA (Fig. 2G). We also tested the effect of the B2 protein of Nodamura virus, a well-characterized viral suppressor of RNAi (VSR) that shields dsRNA from Dicer cleavage (5, 12). SINV-GFP and SINV expressing B2 (SINV-B2) grew to similar levels in baby hamster kidney cells (fig. S4, B and C), Dicer$^{-/-}$aviD$^{-/-}$ cells (fig. S4D), and Dicer$^{+/+}$aviD$^{-/-}$ cells (fig. S4E). In contrast, infectious virion production in Dicer$^{-/-}$aviD$^{+/+}$cells infected with SINV-B2 was greater than in the same cells infected with SINV-GFP by as much as a factor of 100 (fig. S4F). Finally, given the current human impact of the coronavirus pandemic, we further tested the ability to resist infection by severe acute respiratory syndrome coronavirus 2 (SARS-CoV-2) in Dicer$^{+/+}$aviD$^{-/-}$ or

Dicer$^{-/-}$aviD$^{+/+}$ cells, that had been engineered to express the SARS-CoV-2 entry receptor ACE2 (angiotensin-converting enzyme 2) (fig. S2D). We observed a factor of 3 reduction of the number of infected Dicer$^{-/-}$aviD$^{+/+}$ cells relative to infected Dicer$^{+/+}$aviD$^{-/-}$ cells (Fig. 2H). Together, these data reveal that expression of aviD allows for an antiviral RNAi response that restricts replication of several RNA viruses. In contrast, replication of two DNA viruses, vaccinia virus and herpes simplex virus 1, was similar in Dicer$^{+/+}$aviD$^{-/-}$ and Dicer$^{-/-}$aviD$^{+/+}$ cells (fig S4, G and H).

We examined the expression of aviD in mice. aviD transcripts could be detected by fluorescence *in situ* hybridization (fig. S5A) in the crypts of mouse small intestine, where they co-localized with Lgr5, a marker of intestinal stem cells, but were not found in differentiated cells along the villi (Fig. 3A). By PrimeFlow cytometry, validated using complemented Dicer$^{-/-}$aviD$^{-/-}$ HEK293T cells (fig. S5B), *aviD* mRNA was found to be predominantly expressed in a fraction of Lgr5^{+} stem cells in the intestine, as well as in Lgr5^{+} hair follicle stem cells of the skin and in Sox2^{+} neural stem cells of the hippocampus (Fig. 3B). Consistent with the latter, *aviD* expression by RT-qPCR was found in cultured neural stem cells but, unlike *Dicer* mRNA, was lost when the cells were made to differentiate into astrocytes (fig. S5C). These data suggest that aviD is expressed preferentially by stem cells rather than differentiated cells within adult mouse tissues.

To assess the role of aviD in stem cells, we took advantage of an *in vitro* model of organ generation using ES cells. We complemented mouse Dicer$^{-/-}$aviD$^{-/-}$ ES cells (25) with either Dicer or aviD (fig. S6A). The interferon unresponsiveness of ES cells relies in part on their production of miR-673, which inhibits MAVS (mitochondrial antiviral signaling protein) to block coupling of RNA virus detection to IFN gene transcription (2). As a consequence, ES Dicer$^{-/-}$aviD$^{-/-}$ cells lacking miRNAs produce type I interferons and transcribe ISGs in response to viral stimulation, unlike their wild type counterparts (2). We confirmed that introduction of either Dicer or aviD into Dicer$^{-/-}$aviD$^{-/-}$ ES cells restored miRNA production, including that of miR-673, and inhibited the induction of ISGs in response to cell stimulation with a viral RNA mimic (fig. S6, B to E). Complementation with Dicer or aviD additionally suppressed the constitutive activation of protein kinase R (PKR) that has been reported to result from *Dicer* loss (27) and inhibits growth (fig. S7A). Finally, we found that aviD could also mediate dsRNA-induced gene silencing in ES cells (fig. S7B) (19).

Brain organoids derived from ES cells recapitulate the overall organization of the adult brain (28), and Sox2^{+} neural stem cells present in organoids derived from wild type (Dicer$^{+/+}$aviD$^{+/+}$) ES cells expressed more aviD and Dicer transcripts than differentiated cells in the same tissue (fig. S8A). Both Dicer$^{-/-}$aviD$^{+/+}$ and Dicer$^{+/+}$aviD$^{-/-}$ ES cells generated organoids similar to those made by wild type Dicer$^{+/+}$aviD$^{+/+}$ ES cells, including differentiated neuronal layers and astrocytes (fig. S8B). ZIKV infection of brain organoids preferentially targets Sox2^{+} stem cells, resulting in slower organoid growth and increased stem cell demise by apoptosis, which recapitulates the microcephaly phenotype observed in humans (29). Uninfected organoids grew similarly irrespective of genotype (fig. S8C). In contrast, upon infection with ZIKV, Dicer$^{+/+}$aviD$^{-/-}$ organoids grew more slowly than Dicer$^{+/+}$aviD$^{+/+}$ and Dicer$^{-/-}$aviD$^{+/+}$ organoids (Fig. 4A) and produced more

infectious viral particles (Fig. 4B). Thus, despite being expressed at low levels (Fig.1B), endogenous aviD in Dicer$^{+/+}$aviD$^{+/+}$ organoids can display antiviral activity equivalent to that of ectopically-expressed aviD in Dicer$^{-/-}$aviD$^{+/+}$ organoids. Consistent with the notion that absence of aviD compromises stem cell resistance to viral infection, Sox2^{+} stem cells in Dicer$^{+/+}$aviD$^{-/-}$ organoids displayed increased infection with ZIKV (Fig. 4C); accumulated more viral dsRNA, the substrate for aviD (Fig. 4D); and displayed decreased 5-ethynyl-2'-deoxyuridine (EdU) incorporation indicative of lower proliferation (Fig. 4E). ZIKV-derived small RNAs from infected organoids displayed canonical features of viral siRNAs, such as a predominant length of 22 nucleotides (nt) and a read-phasing consistent with the presence of 2-nt 3' overhangs (fig. S9, A to D). Dicer$^{+/+}$aviD$^{-/-}$ organoids showed decreased accumulation of these viral siRNAs (fig. S9B), consistent with impaired ability to restrict ZIKV infection. SARS-CoV-2 can also display brain tropism and infect brain organoids (30). We engineered ES cells to express ACE2 (fig. S8D) and infected organoids with SARS-CoV-2. As for ZIKV infection, the absence of aviD in Dicer$^{+/+}$aviD$^{-/-}$ organoids correlated with an increase in the percentage of virally infected stem cells (Fig. 4F), as well as loss of viral siRNA production (fig S9E). Taken together, these data indicate that aviD can protect adult stem cells from ZIKV and SARS-CoV-2 virus infection by orchestrating an antiviral RNAi response.

Our results show that the *DICER* gene can generate an alternative transcript that encodes aviD, a truncated Dicer that helps protect mouse and human stem cells against RNA virus infection and compensates in part for stem cell hyporesponsiveness to innate IFNs. Our data reveal that mammals, like plants or insects, can produce at least two Dicer proteins, one of which is superior at initiating antiviral RNAi. Interestingly, aviD can also process pre-miRNAs and compensates for Dicer loss in miRNA generation when it is the only isoform expressed in the cell; this would argue that aviD is not fully specialised for antiviral RNAi. Antiviral RNAi has been noted in some studies with differentiated cells, especially when using viruses deficient in VSRs (8–10, 12–14). Whether such observations were due to aviD activity is unknown as our data suggest that aviD is expressed only at low levels in differentiated cells. Why this should be the case is unclear. However, one element to consider is the interplay between antiviral RNAi and the IFN response (5, 19, 20). The action of aviD could deplete infected cells of viral dsRNA, thereby eliminating a key trigger of dsRNA-activated proteins of the IFN response pathway such as RIG-I, MDA5, PKR, or ribonuclease (RNase) L. This is less important for stem cells that are not reliant on the IFN pathway for antiviral resistance. Notably, aviD-mediated antiviral RNAi is not the only defense mechanism in stem cells and likely acts in concert with others conferred by IFN-independent expression of restriction factors encoded by ISGs (21). An aviD-specific knockout mouse will help to delineate the non-redundant contributions of these distinct strategies. Antiviral innate immunity in mammals is therefore a composite of pathways that are tailored to the differentiation status of the cell and that display complementarity as well as redundancy.

Supplementary Material

Refer to Web version on PubMed Central for supplementary material.

Acknowledgements

We thank Pierre Maillard, George Kassiotis, Andreas Wack and members of the Immunobiology laboratory for useful discussions. We are grateful to Anna Baulies Domenech for sharing her protocol for small intestine dissociation and Kevin Ng for his help with ACE2 staining by flow cytometry. We also thank the Crick Flow Cytometry facility for technical assistance, the Crick Advanced Sequencing facility for generating the small RNA libraries, Amelia Acha for help with the BioAnalyzer and Ilaria Dalla Rosa for advice regarding vaccinia virus infection. We are grateful to Lionel Frangeul for help with analysing small RNA libraries, and to Johnathan Canton for help with microscopy analysis. Michael Way kindly provided vaccinia virus. The ZIKV plasmid was a gift from Marco Vignuzzi. Sara Macias and Bryan Cullen kindly provided Dicer$^{-/-}$aviD$^{-/-}$ ES cells and NoDice cells, respectively.

Funding

This work was supported by the Francis Crick Institute which receives core funding from Cancer Research UK (FC001136), the UK Medical Research Council (FC001136), and the Wellcome Trust (FC001136), and by an ERC Advanced Investigator grant (AdG 268670), by a Wellcome Investigator Award (WT106973MA), and a prize from the Louis-Jeantet Foundation. EZP and MDB are supported by EMBO Long-Term Fellowships (ALTF 536-2108 and ALTF 1096-2018) and Marie Skłodowska-Curie Individual Fellowships (832511 and 837951).

Data and materials availability

RNAseq data used for fig. S9 have been deposited in GenBank with the accession number GSE173946. All other data are available in the main text or in the supplementary materials.

References and Notes

1. Goubau D, Deddouche S, Reis e Sousa C. Cytosolic Sensing of Viruses. Immunity. 2013; 38 :855–869. [PubMed: 23706667]
2. Witteveldt J, Knol LI, Macias S. MicroRNA-deficient mouse embryonic stem cells acquire a functional interferon response. eLife. 2019; 8 e44171 [PubMed: 31012846]
3. D'Angelo W, Gurung C, Acharya D, Chen B, Ortolano N, Gama V, Bai F, Guo Y-L. The Molecular Basis for the Lack of Inflammatory Responses in Mouse Embryonic Stem Cells and Their Differentiated Cells. J Immunol. 2017; 198 :2147–2155. [PubMed: 28130495]
4. Hong X-X, Carmichael GG. Innate Immunity in Pluripotent Human Cells: ATTENUATED RESPONSE TO INTERFERON-β. J Biol Chem. 2013; 288 :16196–16205. [PubMed: 23599426]
5. Maillard PV, Veen AG, Poirier EZ, Reis e Sousa C. Slicing and dicing viruses: antiviral RNA interference in mammals. EMBO J. 2019; 38 doi: 10.15252/embj.2018100941
6. Maillard PV, Ciaudo C, Marchais A, Li Y, Jay F, Ding SW, Voinnet O. Antiviral RNA interference in mammalian cells. Science. 2013; 342 :235–238. [PubMed: 24115438]
7. Li Y, Lu J, Han Y, Xiaoxu F, Ding S-W. RNA Interference Functions as an Antiviral Immunity Mechanism in Mammals. Science. 2013; 1241911 :342.
8. Li Y, Basavappa M, Lu J, Dong S, Cronkite DA, Prior JT, Reinecker H-C, Hertzog P, Han Y, Li W-X, Cheloufi S, et al. Induction and suppression of antiviral RNA interference by influenza A virus in mammalian cells. Nat Microbiol. 2016; 2 16250 [PubMed: 27918527]
9. Qiu Y, Xu Y, Zhang Y, Zhou H, Deng Y-Q, Li X-F, Miao M, Zhang Q, Zhong B, Hu Y, Zhang F-C, et al. Human Virus-Derived Small RNAs Can Confer Antiviral Immunity in Mammals. Immunity. 2017; 46 :992–1004. e5 [PubMed: 28636969]
10. Qian Q, Zhou H, Shu T, Mu J, Fang Y, Xu J, Li T, Kong J, Qiu Y, Zhou X. The Capsid Protein of Semliki Forest Virus Antagonizes RNA Interference in Mammalian Cells. J Virol. 2019; 94 e01233-19
11. Xu Y-P, Qiu Y, Zhang B, Chen G, Chen Q, Wang M, Mo F, Xu J, Wu J, Zhang R-R, Cheng M-L, et al. Zika virus infection induces RNAi-mediated antiviral immunity in human neural progenitors and brain organoids. Cell Res. 2019; doi: 10.1038/s41422-019-0152-9
12. Han Q, Chen G, Wang J, Jee D, Li W-X, Lai EC, Ding S-W. Mechanism and Function of Antiviral RNA Interference in Mice. mBio. 2020; 11 e03278-19 [PubMed: 32753500]

13. Zhang Y, Li Z, Ye Z, Xu Y, Wang B, Wang C, Dai Y, Lu J, Lu B, Zhang W, Li Y. The activation of antiviral RNA interference not only exists in neural progenitor cells but also in somatic cells in mammals. Emerg Microbes Infect. 2020; 9 :1580–1589. [PubMed: 32576094]
14. Qiu Y, Xu Y-P, Wang M, Miao M, Zhou H, Xu J, Kong J, Zheng D, Li R-T, Zhang R-R, Guo Y, et al. Flavivirus induces and antagonizes antiviral RNA interference in both mammals and mosquitoes. Sci Adv. 2020; 6 eaax7989 [PubMed: 32076641]
15. Cullen BR, Cherry S, tenOever BR. Is RNA Interference a Physiologically Relevant Innate Antiviral Immune Response in Mammals? Cell Host Microbe. 2013; 14 :374–378. [PubMed: 24139396]
16. Schuster S, Tholen LE, Overheul GJ, van Kuppeveld FJM, van Rij RP. Deletion of Cytoplasmic Double-Stranded RNA Sensors Does Not Uncover Viral Small Interfering RNA Production in Human Cells. mSphere. 2017; 2 e00333-17 [PubMed: 28815217]
17. Tsai K, Courtney DG, Kennedy EM, Cullen BR. Influenza A virus-derived siRNAs increase in the absence of NS1 yet fail to inhibit virus replication. RNA. doi: 10.1261/rna.066332.118
18. Schuster S, Overheul GJ, Bauer L, van Kuppeveld FJM, van Rij RP. No evidence for viral small RNA production and antiviral function of Argonaute 2 in human cells. Sci Rep. 2019; 9
19. Maillard PV, Van der Veen AG, Deddouche-Grass S, Rogers NC, Merits A, Reis e Sousa C. Inactivation of the type I interferon pathway reveals long double-stranded RNA-mediated RNA interference in mammalian cells. EMBO J. 2016; 35 :2505–2518. [PubMed: 27815315]
20. van der Veen AG, Maillard PV, Schmidt JM, Lee SA, Deddouche-Grass S, Borg A, Kjær S, Snijders AP, Reis e Sousa C. The RIG-I-like receptor LGP2 inhibits Dicer-dependent processing of long double-stranded RNA and blocks RNA interference in mammalian cells. EMBO J. 2018 e97479 [PubMed: 29351913]
21. Wu X, Dao Thi VL, Huang Y, Billerbeck E, Saha D, Hoffmann H-H, Wang Y, Silva LAV, Sarbanes S, Sun T, Andrus L, et al. Intrinsic Immunity Shapes Viral Resistance of Stem Cells. Cell. 2017; doi: 10.1016/j.cell.2017.11.018
22. Ma E, MacRae IJ, Kirsch JF, Doudna JA. Autoinhibition of Human Dicer by Its Internal Helicase Domain. J Mol Biol. 2008; 380 :237–243. [PubMed: 18508075]
23. Kennedy EM, Whisnant AW, Kornepati AVR, Marshall JB, Bogerd HP, Cullen BR. Production of functional small interfering RNAs by an amino-terminal deletion mutant of human Dicer. Proc Natl Acad Sci. 2015; 112 E6945-E6954 [PubMed: 26621737]
24. Flemr M, Malik R, Franke V, Nejepinska J, Sedlacek R, Vlahovicek K, Svoboda P. A Retrotransposon-Driven Dicer Isoform Directs Endogenous Small Interfering RNA Production in Mouse Oocytes. Cell. 2013; 155 :807–816. [PubMed: 24209619]
25. Babiarz JE, Ruby JG, Wang Y, Bartel DP, Blelloch R. Mouse ES cells express endogenous shRNAs, siRNAs, and other Microprocessor-independent, Dicer-dependent small RNAs. Genes Dev. 2008; 22 :2773–2785. [PubMed: 18923076]
26. Bogerd HP, Whisnant AW, Kennedy EM, Flores O, Cullen BR. Derivation and characterization of Dicer- and microRNA-deficient human cells. RNA. 2014; 20 :923–937. [PubMed: 24757167]
27. Gurung C, Fendereski M, Sapkota K, Guo J, Huang F, Guo Y-L. Dicer represses the interferon response and the double-stranded RNA-activated protein kinase pathway in mouse embryonic stem cells. J Biol Chem. 2021; 296 100264 [PubMed: 33837743]
28. Lancaster MA, Renner M, Martin C-A, Wenzel D, Bicknell LS, Hurles ME, Homfray T, Penninger JM, Jackson AP, Knoblich JA. Cerebral organoids model human brain development and microcephaly. Nature. 2013; 501 :373–379. [PubMed: 23995685]
29. Garcez PP, Loiola EC, Higa LM, Trindade P, Delvecchio R, Nascimento JM, Brindeiro R, Tanuri A, Rehen SK. Zika virus impairs growth in human neurospheres and brain organoids. :4.
30. Iadecola C, Anrather J, Kamel H. Effects of COVID-19 on the Nervous System. Cell. 2020; 183 :16–27. e1 [PubMed: 32882182]
31. McKnight KL, Simpson DA, Lin S-C, Knott TA, Polo JM, Pence DF, Johannsen DB, Heidner HW, Davis NL, Johnston RE. Deduced consensus sequence of Sindbis virus strain AR339: mutations contained in laboratory strains which affect cell culture and in vivo phenotypes. J Virol. 1996; 70 :1981–1989. [PubMed: 8627724]

32. Schwarz MC, Sourisseau M, Espino MM, Gray ES, Chambers MT, Tortorella D, Evans MJ. mSphere. doi: 10.1128/mSphere.00246-16
33. Saleh M-C, Tassetto M, van Rij RP, Goic B, Gausson V, Berry B, Jacquier C, Antoniewski C, Andino R. Antiviral immunity in Drosophila requires systemic RNA interference spread. Nature. 2009; 458 :346–350. [PubMed: 19204732]
34. Maillard PV, Van der Veen AG, Deddouche-Grass S, Rogers NC, Merits A, Reis e Sousa C. Inactivation of the type I interferon pathway reveals long double-stranded RNA-mediated RNA interference in mammalian cells. EMBO J. 2016; 35 :2505–2518. [PubMed: 27815315]
35. van der Veen AG, Maillard PV, Schmidt JM, Lee SA, Deddouche-Grass S, Borg A, Kjær S, Snijders AP, Reis e Sousa C. The RIG-I-like receptor LGP2 inhibits Dicer-dependent processing of long double-stranded RNA and blocks RNA interference in mammalian cells. EMBO J. 2018 e97479 [PubMed: 29351913]
36. Velasco S, Kedaigle AJ, Simmons SK, Nash A, Rocha M, Quadrato G, Paulsen B, Nguyen L, Adiconis X, Regev A, Levin JZ, et al. Individual brain organoids reproducibly form cell diversity of the human cerebral cortex. Nature. 2019; 570 :523–527. [PubMed: 31168097]
37. Gracz, AD, Puthoff, BJ, Magness, ST. Somatic Stem CellsMethods in Molecular Biology. Singh, SR, editor. Vol. 879. Humana Press; Totowa, NJ: 2012. 89–107.
38. Gracz AD, Fuller MK, Wang F, Li L, Stelzner M, Dunn JCY, Martin MG, Magness ST. Brief report: CD24 and CD44 mark human intestinal epithelial cell populations with characteristics of active and facultative stem cells: FACS Enrichment of Human Intestinal Stem Cells. STEM CELLS. 2013; 31 :2024–2030. [PubMed: 23553902]
39. Cardoso A, Gil Castro A, Martins AC, Carriche GM, Murigneux V, Castro I, Cumano A, Vieira P, Saraiva M. The Dynamics of Interleukin-10-Afforded Protection during Dextran Sulfate Sodium-Induced Colitis. Front Immunol. 2018; 9 :400. [PubMed: 29545807]
40. Lancaster MA, Corsini NS, Wolfinger S, Gustafson EH, Phillips AW, Burkard TR, Otani T, Livesey FJ, Knoblich JA. Guided self-organization and cortical plate formation in human brain organoids. Nat Biotechnol. 2017; 35 :659–666. [PubMed: 28562594]
41. Martin M. Cutadapt removes adapter sequences from high-throughput sequencing reads. EMBnet journal. 2011; 17 :10.
42. Langmead B, Trapnell C, Pop M, Salzberg SL. Ultrafast and memory-efficient alignment of short DNA sequences to the human genome. Genome Biol. 2009; 10 :R25. [PubMed: 19261174]
43. Li H, Handsaker B, Wysoker A, Fennell T, Ruan J, Homer N, Marth G, Abecasis G, Durbin R. 1000 Genome Project Data Processing Subgroup, The Sequence Alignment/Map format and SAMtools. Bioinformatics. 2009; 25 :2078–2079. [PubMed: 19505943]
44. Quinlan AR, Hall IM. BEDTools: a flexible suite of utilities for comparing genomic features. Bioinformatics. 2010; 26 :841–842. [PubMed: 20110278]
45. Lemon J. Plotrix: A Package in the Red Light District of R. R-News. 6 :8–12.
46. Gurung C, Fendereski M, Sapkota K, Guo J, Huang F, Guo Y-L. Dicer represses the interferon response and the double-stranded RNA-activated protein kinase pathway in mouse embryonic stem cells. J Biol Chem. 2021; 296 100264 [PubMed: 33837743]

Europe PMC Funders Author Manuscripts

One sentence summary

Mammalian stem cells thwart RNA virus infection by expressing an isoform of Dicer that potentiates antiviral RNAi

Europe PMC Funders Author Manuscripts

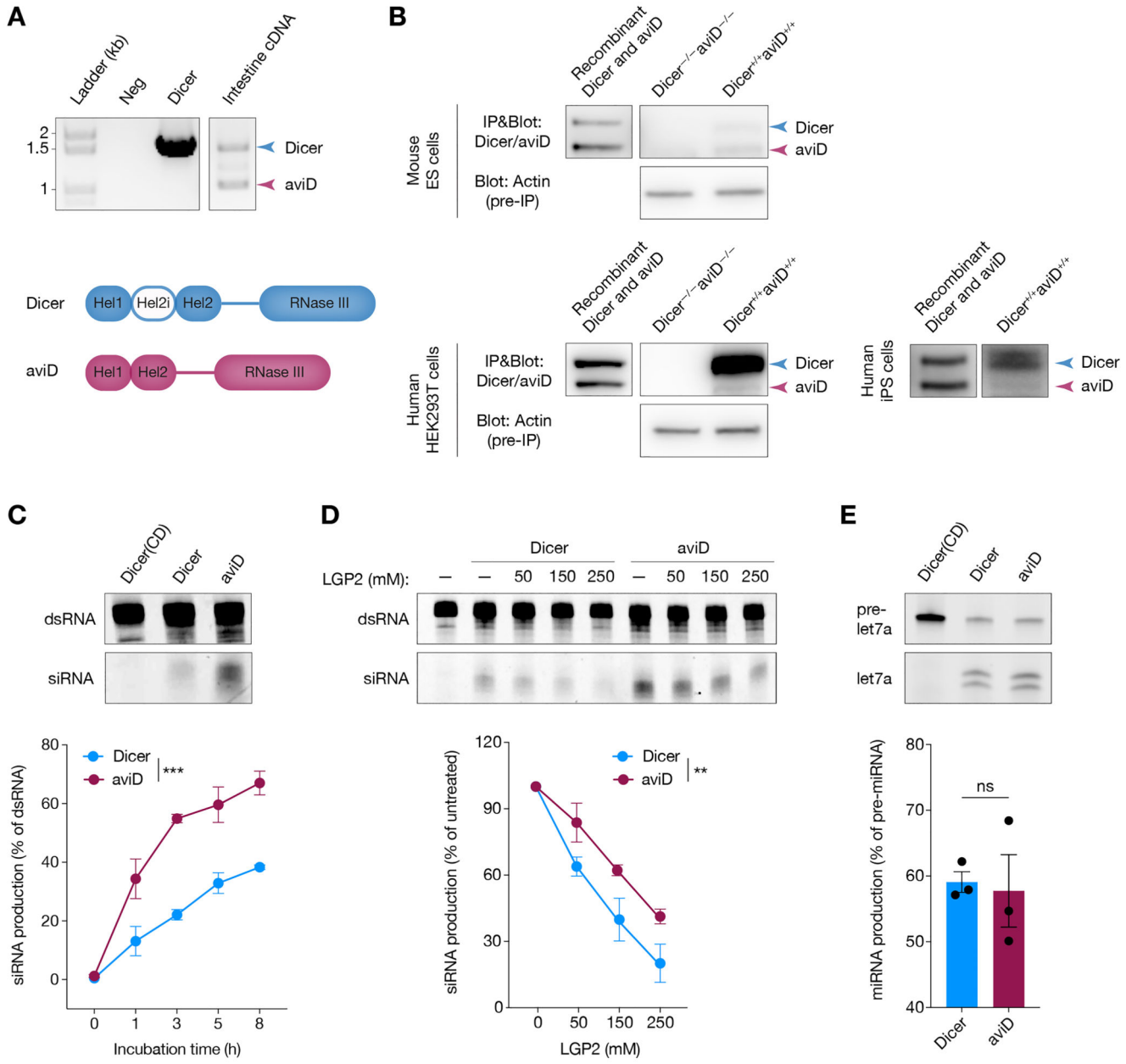

Figure 1. aviD is an isoform of Dicer that efficiently cleaves dsRNA.

(**A**) Dicer PCR amplicons using vehicle (Neg), a plasmid coding for Dicer, or mouse small intestine cDNA templates. In addition to a canonical product corresponding to full-length Dicer, an in-frame transcript missing exons 7 and 8 (nucleotides 705 to 1346 of the coding sequence) was detected. This corresponds to an isoform termed antiviral Dicer (aviD) lacking the Hel2i domain of the helicase (white). (**B**) Immunoblots from wild type Dicer$^{+/+}$aviD$^{+/+}$ or Dicer$^{-/-}$aviD$^{-/-}$ mouse ES cell, HEK293T cell or Dicer$^{+/+}$aviD$^{+/+}$ human iPSC lysates before (pre-IP) or after immunoprecipitation with a Dicer/aviD specific antibody. Recombinant Flag-tagged Dicer and aviD were included as controls. (**C**) Recombinant Flag-tagged Dicer, Dicer catalytically-deficient [Dicer(CD), used as a

negative control] or aviD was incubated with synthetic Cy5-labelled dsRNA at 37oC for the indicated time. The reactions were resolved on a denaturing polyacrylamide gel, visualised by Cy5 in-gel fluorescence and Dicer vs aviD cleavage quantitated by densitometry. (**D**) Increasing concentrations of recombinant LGP2 were added to the *in vitro* dicing reaction as in (C) and incubated 3 h at 37oC. After densitometric quantitation, siRNA amount was normalized to the amount of siRNA produced in a reaction without LGP2. (**E**) Immunopurified Flag-tagged Dicer, Dicer catalytically-deficient [Dicer(CD)] or aviD, were incubated with let-7a pre-miRNA at 37oC for 20 min. The reactions were resolved on a denaturing polyacrylamide gel, visualised by Cy5 in-gel fluorescence and Dicer vs aviD cleavage quantitated by densitometry. Data in C-E are pooled from three independent experiments and are plotted as mean ± SEM. ns, not significant; **p < 0.01, ***p < 0.001 (two-way ANOVA [C,D] and Mann-Whitney test [E]).

Europe PMC Funders Author Manuscripts

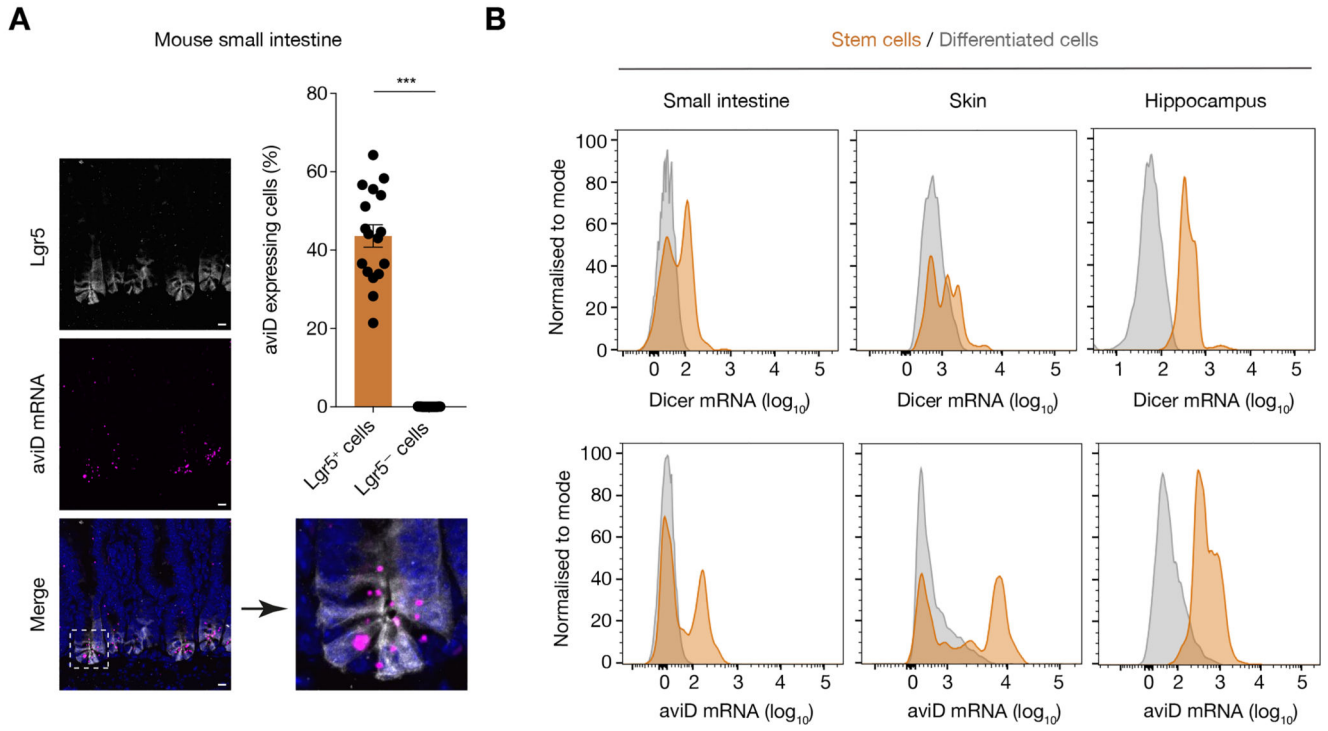

Figure 2. aviD can mediate antiviral RNAi.

(**A-B**) HEK293T Dicer$^{-/-}$aviD$^{-/-}$ cells complemented with Dicer (Dicer$^{+/+}$aviD$^{-/-}$) or aviD (Dicer$^{-/-}$aviD$^{+/+}$) were infected with SINV (A) or ZIKV (B) at MOI 0.1. Supernatant was collected at the indicated times points and viral content determined by plaque assay. (**C-E**) HEK293T Dicer$^{-/-}$aviD$^{-/-}$ cells induced by doxocycline to express Flag-Dicer (C), aviD (D), or catalytically-deficient aviD [aviD(CD)] (E) were infected with SINV-GFP. Flow cytometry was used to monitor the expression of Dicer/aviD via anti-Flag staining and SINV replication via GFP fluorescence. (**F**) Representative contour plots from 16 h post infection. Boxes represent Flag positive cells defined on the basis of the uninduced controls (top left plot). (**G**) Dicer$^{+/+}$aviD$^{-/-}$or Dicer$^{-/-}$aviD$^{+/+}$ HEK293T cells were transfected with siRNA targeting Ago2 (siAgo2) or with control siRNA (siCt) and infected with ZIKV at MOI 0.1. Supernatant was collected at the indicated time points and viral content was determined by plaque assay. (**H**) Immunofluorescence of Dicer$^{-/-}$aviD$^{+/+}$ Dicer$^{+/+}$aviD$^{-/-}$ HEK293T cells expressing ACE2 infected with SARS-CoV-2 and stained for SARS-CoV-2 N protein (magenta) and dsRNA (white). Scale bar: 20 μm. Graph shows percentage of infected cells. Data in A-H are from one of three independent experiments. Data points represent mean ± SEM, $n = 3$ biological replicates. ns, not significant; *p < 0.05, **p < 0.01, ***p < 0.001. (two-way ANOVA [A-E,G], unpaired t-test [H]).

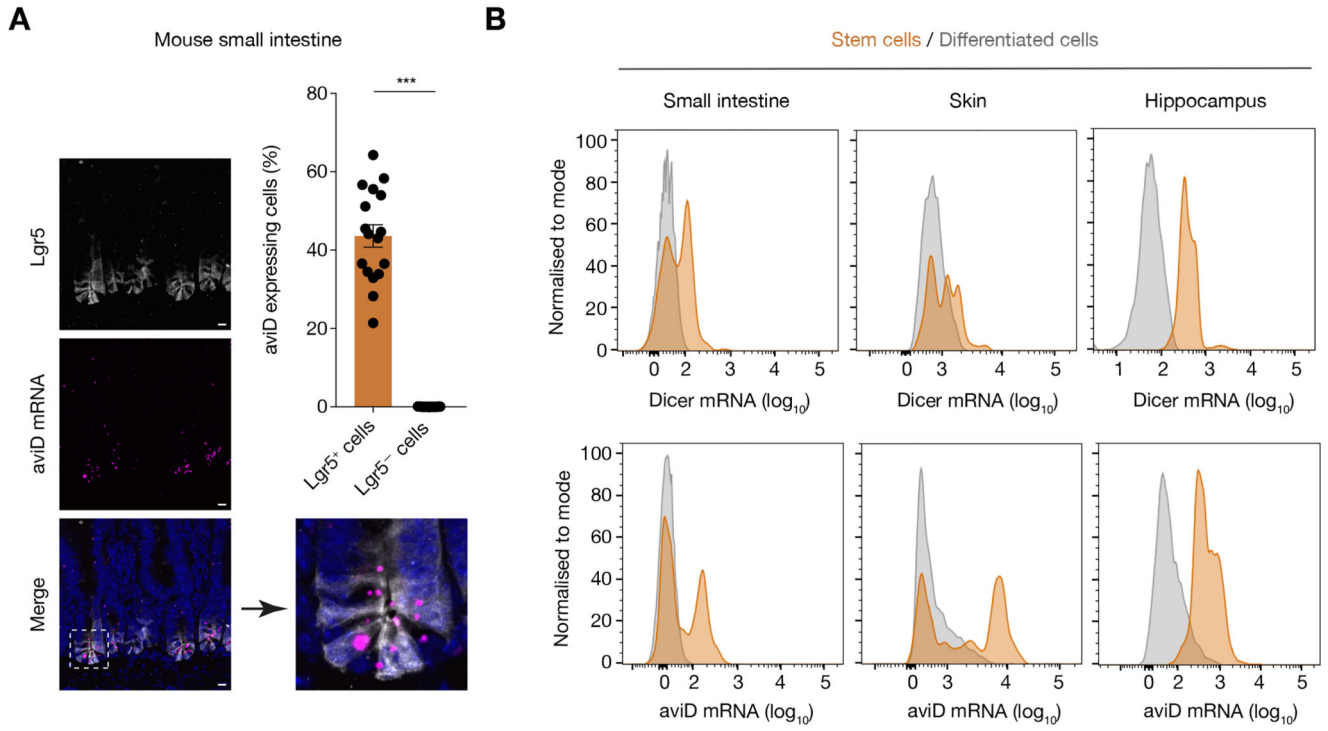

Figure 3. *aviD* is enriched in tissue stem cells.

(**A**) Small intestine from an Lgr5-GFP reporter mouse was fixed, sectioned and probed for aviD mRNA (magenta) by fluorescence *in situ* hybridisation. The aviD probe was designed to detect the exon-exon junction specific to aviD and cannot detect Dicer mRNA (Fig. S5A). $Lgr5^+$ stem cells were identified with anti-GFP (white) and nuclei were visualized by DNA staining (Hoechst, blue). Scale bar: 30 μm. Percentage of stem ($Lgr5^+$) or differentiated ($Lgr5^—$) cells expressing aviD mRNA was determined on 17 images with at least three villi each. Data points represent mean and error bars are SEM. Mann-Whitney test, ***$p < 0.001$. (**B**) aviD or Dicer mRNA was measured by PrimeFlow cytometry in stem ($Lgr5^+$) or differentiated ($Lgr5^—$) cells from small intestine or skin isolated from Lgr5-GFP reporter mice or in stem or differentiated cells from hippocampus distinguished by the presence or absence of Sox2 mRNA, respectively.

Europe PMC Funders Author Manuscripts

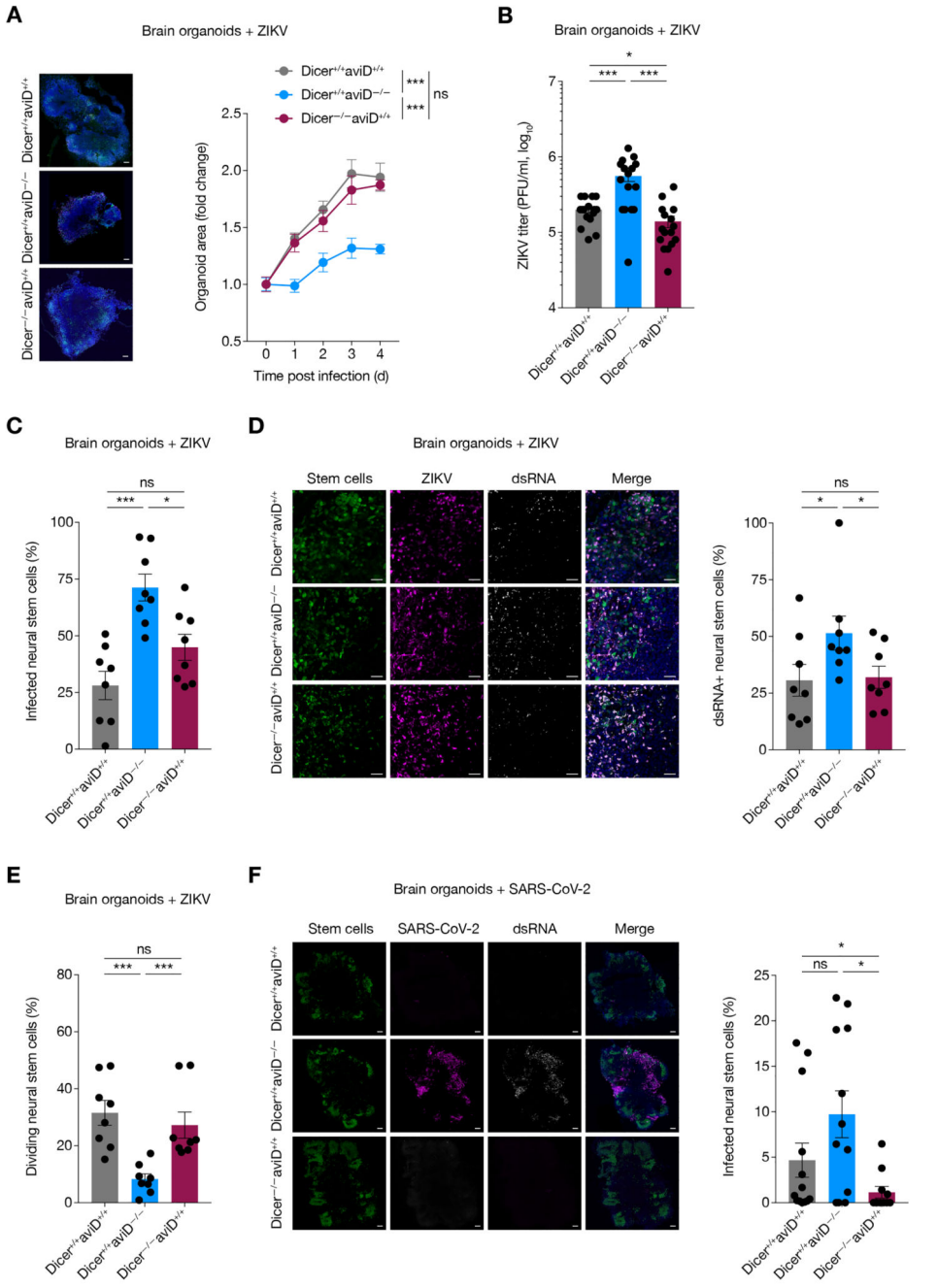

Figure 4. aviD thwarts viral infection in stem cells.

(**A**) Individual Dicer$^{+/+}$aviD$^{+/+}$, Dicer$^{+/+}$aviD$^{—/—}$ or Dicer$^{—/—}$aviD$^{+/+}$ brain organoids were infected with ZIKV and organoid area was monitored for 4 days. Immunofluorescent stanining and confocal microscopy on organoid sections was carried out to identify stem cells by Sox2 expression (green) and infected cells by ZIKV glycoprotein expression (magenta). Scale bar: 100 μm. (**B**) Production of viral particles from ZIKV-infected organoids was determined by transferring individual organoids into fresh medium at day 3 post infection and collecting the supernatant 24 hours thereafter to determine viral content

by plaque assay. (**C**) Percentage of ZIKV-infected stem cells was measured at 4 days post infection by immunofluorescence on organoids sections. (**D**) dsRNA in infected stem cells was visualised by immunofluorescence on organoid sections after 4 days of infection. Images show dsRNA (gray) in ZIKV-infected (magenta) stem cells (green). Scale bar: 20 μm. (E) Stem cell division rate was measured by pulsing organoids with EdU at day 3 for 1 h and chasing for 24 h. Organoids section were analysed by immunofluorescence, with Sox2 staining identifying stem cells and EdU staining marking cells in S phase at time of pulsing. (**F**) $Dicer^{+/+}aviD^{+/+}$, $Dicer^{+/+}aviD^{-/-}$ or $Dicer^{-/-}aviD^{+/+}$ brain organoids expressing ACE2 were infected with SARS-CoV-2 for 48 h. Percentage of infected stem cells was determined by immunofluorescence on sections stained for the stem cell marker Sox2 (green) and for the SARS-CoV-2 N protein (magenta). Scale bar: 100 μm. In A-F, mean and SEM are shown. [A,B] $n = 16$ organoids per condition. [C,D,E] $n = 8$ organoids per condition, 8 with highest fold change in area at day 4 for $Dicer^{+/+}aviD^{+/+}$ and $Dicer^{-/-}aviD^{+/+}$, 8 with lowest fold change in area for $Dicer^{+/+}aviD^{-/-}$. [F] $n = 11$ organoids per condition. ns, not significant; *p < 0.05. ***p < 0.001 (two-way ANOVA [A], Mann-Whitney test [B-F]).